



Synthesis and properties of trifluoromethoxyl fluoroformyl anhydride, $\text{CF}_3\text{OC}(\text{O})\text{OC}(\text{O})\text{F}$

Martín M. Manetti, Gustavo A. Argüello, Maxi A. Burgos Paci *

Instituto de Investigaciones en Físico Química de Córdoba (INFIQC) CONICET-UNC, Departamento, de Físico Química, Facultad de Ciencias Químicas, Universidad Nacional de Córdoba, Ciudad, Universitaria, X5000HUA Córdoba, Argentina

ARTICLE INFO

Article history:

Received 9 March 2012

Received in revised form 17 May 2012

Accepted 21 May 2012

Available online 12 June 2012

Keywords:

Fluorinated radicals

Gas phase reaction mechanism

Perfluorinated anhydride

DFT calculations

ABSTRACT

In the present work the synthesis of the trifluoromethoxyl fluoroformyl anhydride is presented for the first time. Two strategies were employed to obtain $\text{CF}_3\text{OC}(\text{O})\text{OC}(\text{O})\text{F}$: the thermal decomposition of $\text{CF}_3\text{OC}(\text{O})\text{OOC}(\text{O})\text{F}$ in excess of CO, and the reaction between $\text{CF}_3\text{OC}(\text{O})\text{OOC}(\text{O})\text{F}$, $\text{FC}(\text{O})\text{OOC}(\text{O})\text{F}$ and CO. A mechanism was proposed taking into account reaction rates and thermal stability of the intermediates. DFT calculations at B3LYP/6-311+G* level were used to explore the conformational space of this molecule and the relative populations of conformers at room temperature, and to simulate the experimental vibrational spectrum. This molecule completes the family of the asymmetric oxygen bonded acyl compounds $\text{CF}_3\text{OC}(\text{O})\text{-Ox-C}(\text{O})\text{F}$ with $x = 1\text{-}3$.

© 2012 Elsevier B.V. All rights reserved.

1. Introduction

Research on fluorinated carbo-oxygenated compounds is highly attractive for several reasons, among which are the applications of fluorinated ethers, olefins, and fluoropolymers in the broad spectrum of industries related with optics, petrochemistry, aerospace, etc. [1,2]. Besides, study of these compounds is of importance in atmospheric chemistry to get a deeper understanding of the tropospheric and stratospheric fate of CFCs substitutes. Following this line of research, synthesis and characterization of several acyl anhydrides, peroxides, and trioxides have been achieved in the last years. The families of compounds where two $\text{RC}(\text{O})\text{-}$ groups are bounded by one, two, or three oxygen atoms are known for the symmetric molecules ($x = 1\text{-}3$) $\text{FC}(\text{O})\text{-Ox-C}(\text{O})\text{F}$ [3–5], and $\text{CF}_3\text{OC}(\text{O})\text{-Ox-C}(\text{O})\text{OCF}_3$ [6–8]. The asymmetric compounds $\text{CF}_3\text{OC}(\text{O})\text{-Ox-C}(\text{O})\text{F}$ with two and three oxygen atoms are already known [9,10] but their isolation was rather difficult. They were studied by gas electron diffraction, vibrational spectroscopy, thermal properties, etc. [11–15].

Perfluorinated acyloxy compounds are formed mainly by gas phase photolysis of CF_3 and/or FCO radical precursors in excess of CO and O_2 (an exception is the synthesis of $\text{FC}(\text{O})\text{OOC}(\text{O})\text{F}$ obtained from a $\text{F}_2/\text{O}_2/\text{CO}$ mixture). The temperature at which the photolysis is carried out is of central importance to stabilize the different carboxy radicals CF_3OCOx and FCOx , $x = 1\text{-}3$ that will recombine to

produce different species. In the case of the symmetric anhydride $\text{CF}_3\text{OC}(\text{O})\text{OC}(\text{O})\text{OCF}_3$, it is obtained from decomposition of the parent trioxide [6]. The same strategy was followed to synthesize the asymmetric molecule trifluoromethoxyl fluoroformyl anhydride, $\text{CF}_3\text{OC}(\text{O})\text{OC}(\text{O})\text{F}$. In this paper we present for the first time the synthesis of this compound besides the analysis of its vibrational spectrum and DFT calculations of the ground state potential energy surface. The title molecule is the anhydride that completes the family of the asymmetric oxygen bonded acyl compounds $\text{CF}_3\text{OC}(\text{O})\text{-Ox-C}(\text{O})\text{F}$ with $x = 1\text{-}3$.

2. Materials and methods

The polyoxides $\text{CF}_3\text{OC}(\text{O})\text{OOC}(\text{O})\text{F}$ and $\text{CF}_3\text{OC}(\text{O})\text{OC}(\text{O})\text{F}$ are potentially explosive, especially in the presence of oxidizable materials. All reactions should be carried out in millimolar quantities only, and it is important to take safety precautions especially when these compounds are handled in liquid and solid state.

Commercially available samples of perfluoroacetic anhydride $\text{CF}_3\text{C}(\text{O})\text{OC}(\text{O})\text{CF}_3$ (PCR), CO (PRAXAIR), and O_2 (AGA) were used. Dry oxygen was obtained from liquified oxygen at atmospheric pressure in a trap immersed in liquid air and then transferred to the reactor up to obtain the desired pressure. $\text{FC}(\text{O})\text{C}(\text{O})\text{F}$ was prepared by fluorination of oxalyl chloride [16].

Volatile materials were manipulated in a glass vacuum line equipped with two capacitance pressure gauges (0–760 Torr, MKS Baratron; 0–70 mbar, Bell and Howell), three U traps, and valves with poly(tetrafluoroethylene) stems (Young, London).

* Corresponding author. Tel.: +54 351 4334180.

E-mail address: mburgos@fcq.unc.edu.ar (M.A.B. Paci).

The vacuum line was connected to the photoreactor (12 L round flask equipped with a low pressure Hg Lamp – 254 nm) and to an IR gas cell (double-walled quartz with Si windows, optical path length 210 mm) placed in the sample compartment of a Fourier transform infrared (FT-IR) spectrometer (Bruker IFS 66v). The spectra were taken with a resolution of 2 cm⁻¹ and the addition of 4 interferometer scans. This arrangement made it possible to follow the course of the synthesis.

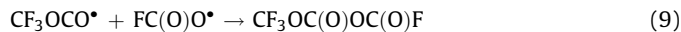
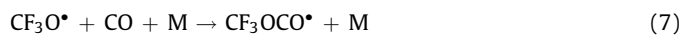
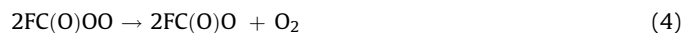
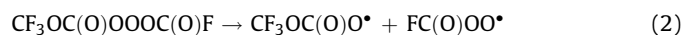
3. Theoretical calculations

The conformational space of the ground electronic state of CF₃OC(O)OC(O)F was studied using the density functional theory (DFT). The geometries of all conformers were optimized using the hybrid density functional B3LYP with the 6-311+G* basis set. Additionally, harmonic vibrational frequencies and zero-point energies (ZPE) were calculated at the same level of theory to check whether the obtained stationary points were either isomers or first-order transition states; the calculated conformers possessed no imaginary frequencies. The determination of the Hessian matrix also enabled calculation of the thermochemical quantities for the conformers at 298.15 K. The selected DFT method has been extensively applied to the determination of geometric parameters of related fluoro-carbon-oxygenated compounds, yielding accurate results tested with gas electron diffraction experiments [13,14,17]. Since we are interested in the minima of the potential energy surface, and DFT methods take into account the electron correlation energy to a partial extent [18], we think that the B3LYP/6-311+G* method should be adequate to describe the relative energies for the isomers. All symmetry restrictions were turned off in the calculations. The GAUSSIAN03 program package [19] was used in conjunction with Molden 4.1 [20].

4. Results and discussion

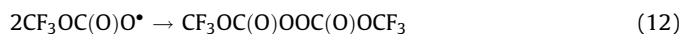
4.1. Synthesis method

The title molecule was obtained from the recombination of CF₃OCO and FCO₂ radicals produced in the reaction chamber from thermal decomposition of CF₃OC(O)OOOC(O)F in excess of CO. The complete method of synthesis for the parent trioxide is described elsewhere [10]. Briefly, it is obtained from the 266 nm photolysis of trifluoroacetic anhydride (CF₃C(O)OC(O)CF₃) and oxalyl fluoride (FC(O)C(O)F) in excess of CO and O₂ at about 223 K. Once the asymmetric trioxide is formed, the lamp is turned off and the reactor bath is cooled down to about 193 K. At this temperature the trioxide sticks on the reactor walls and the remaining products and starting materials such as CF₂O, CO₂, CF₃C(O)F, CF₃OOFCF₃, FC(O)OOC(O)F, CO, and O₂ can be pumped out. After this, CO is introduced in the reactor and the ethanol bath is allowed to slowly warm up. In this way, the trioxide sublimates, and when temperature reaches 253 K the dissociation of the molecule starts according to reactions (1) and (2) producing CF₃OC(O)Ox and FCOx radicals that, in excess of CO, will give rise to the formation of CF₃OC(O)OC(O)F. The proposed mechanism is detailed from reactions (1)–(10) as follows:



Reaction (10) is rather speculative because it involves FCO[•] radicals whose formation is difficult at the temperatures of this system, taking into account that FCO should come from the decarboxylation of FC(O)O, with a rate constant of $k_6 = 0.22 \text{ s}^{-1}$ [21] followed by reaction (8). In comparison, the decarboxylation of CF₃OC(O)O, $k_5 = 35 \text{ s}^{-1}$ [22], is 160 times faster.

The expected products besides the anhydride are those shown in reactions (9)–(14), which correspond to termination steps:



Once the reaction is terminated, the gas mixture is directed through three U-traps kept at 77 K in dynamic vacuum. In this way, the products are trapped but the remaining CO is pumped off. In order to purify and identify the products, they were collected in a glass trap connected before the U-traps. The temperatures of the U-traps were set up 193, 153, and 77 K and the sample was pumped through the traps. The most volatile products, retained in the 77 K trap, were identified as CF₂O, CO₂, and a small amount of FC(O)OOC(O)F and discarded. At 153 K a blend of the peroxides FC(O)OOC(O)F, CF₃OC(O)OOC(O)F, and CF₃OC(O)OOC(O)OCF₃ was identified. CF₃OC(O)OOC(O)F, CF₃OC(O)OOC(O)OCF₃, CF₃OC(O)OC(O)OCF₃, and CF₃OC(O)OC(O)F were found in the last U trap at 193 K. Peroxides were separated from anhydrides by static distillation at about 243 K. Both anhydrides CF₃OC(O)OC(O)OCF₃ and CF₃OC(O)OC(O)F have similar vapor pressure and it is not possible to separate them by distillation.

Another strategy for the synthesis of CF₃OC(O)OC(O)F was the reaction between CF₃OC(O)OOC(O)F from our own repository, FC(O)OOC(O)F, and CO. Under these conditions, formation of CF₃OC(O)OC(O)OCF₃ is avoided. The experiment was conducted in a 1L round glass flask filled with 30 mbar of CF₃OC(O)OOC(O)F, 15 mbar of FC(O)OOC(O)F and CO to reach 500 mbar of total pressure. The flask was immersed in a water bath at 333 K. At this temperature the unimolecular decomposition of CF₃OC(O)OOC(O)F and FC(O)OOC(O)F:



has rate constants of $k_{-13} = 2.9 \times 10^{-4} \text{ s}^{-1}$ [23] and $k_{-11} = 1.9 \times 10^{-3} \text{ s}^{-1}$ [15] respectively. The former peroxide decomposes into CF₃OC(O)O[•] and FC(O)O[•] radicals according to (-13), but CF₃OC(O)O[•] decarboxylates very fast to give CF₃O[•] and CO₂. CF₃O[•] reacts efficiently with CO to give CF₃OCO[•] and its combination with FC(O)O[•] yields the desired anhydride. It is worth noting that the formation of CF₃OC(O)OC(O)OCF₃ is inhibited by the decarboxylation rate of CF₃OC(O)O[•] at 333 K and the relative amount of FC(O)O[•] with respect to CF₃OCO[•].

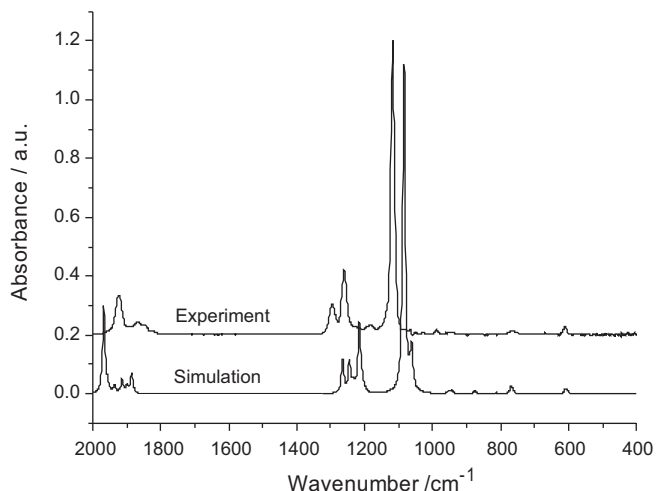


Fig. 1. Experimental and calculated MIR spectrum of $\text{CF}_3\text{OC}(\text{O})\text{OC}(\text{O})\text{F}$. Simulated spectrum is the result of adding the three most stable conformers at the populations shown in Table 1.

The evolution of the reaction was followed by measuring the IR absorbance of $\text{CF}_3\text{OC}(\text{O})\text{OC}(\text{O})\text{F}$ ($\sigma_{1152} = 6.7 \times 10^{-18} \text{ cm}^2 \text{ molecule}^{-1}$). Once the reaction was terminated, the gas mixture was condensed with liquid nitrogen in the U-traps. The low-temperature distillation gave CF_2O and SiF_4 at 81 K, $\text{FC}(\text{O})\text{OOC}(\text{O})\text{F}$ at 193 K and pure $\text{CF}_3\text{OC}(\text{O})\text{OC}(\text{O})\text{F}$ (>99%) remained at 225 K. Fig. 1 shows the IR spectrum of the molecule obtained with a 2 cm^{-1} resolution.

Table 1

B3LYP/6-311+G* absolute and relative energies plus ZPE for the six conformers found for $\text{CF}_3\text{OC}(\text{O})\text{OC}(\text{O})\text{F}$.

Conformer	$E+\text{ZPE}$ (H)	$\Delta E+\text{ZPE}$ (kcal mol $^{-1}$)	Relative population (%) at 298 K
s-s-s	-814.804749	0	77.38
s-a-s	-814.803011	1.09	12.28
s-s-a	-814.802679	1.3	8.64
a-s-s	-814.800631	2.58	0.99
s-a-a	-814.800112	2.91	0.57
a-s-a	-814.798763	3.76	0.14

4.2. Calculations

The conformational space of $\text{CF}_3\text{OC}(\text{O})\text{OC}(\text{O})\text{F}$ can be described through the four main torsion angles of the skeleton $\text{F}-\text{C}(\text{F}_2)-\text{O}-\text{C}(\text{O})-\text{O}-\text{C}(\text{F})=\text{O}$, which in turn can be conveniently reduced to three because $\varphi_0(\text{F}-\text{C}(\text{F}_2)-\text{O}-\text{C}(\text{O}))$ always adopts the anti configuration. These three main dihedrals can adopt either anti ($\sim 180.0^\circ$) or syn ($\sim 0.0^\circ$) configurations (i) the relative position of the CF_3 group to the $\text{C}=\text{O}$ bond, $\varphi_1(\text{F}_3\text{C}-\text{O}-\text{C}=\text{O})$; and (ii) the relative position of each double bond to the anhydride bridge $-\text{O}-$, $\varphi_2(\text{O}=\text{C}-\text{O}-\text{COF})$ and $\varphi_3(\text{C}-\text{O}-\text{CF}=\text{O})$ respectively. Enantiomeric forms are not taken into account since there are no energy differences between them. The different conformers are designated according to the letter code “a” (anti) or “s” (syn) for $\varphi_1 \varphi_2 \varphi_3$ in the sequence $\varphi_1-\varphi_2-\varphi_3$. Six minima were found in the B3LYP/6-311+G* PES being the s-s-s the most stable conformer. Eight minima are possible according to the possibilities of the dihedrals; however, in the a-a-a and a-a-s conformers the CF_3 fragment overlaps the COF being both configurations not at a minimum.

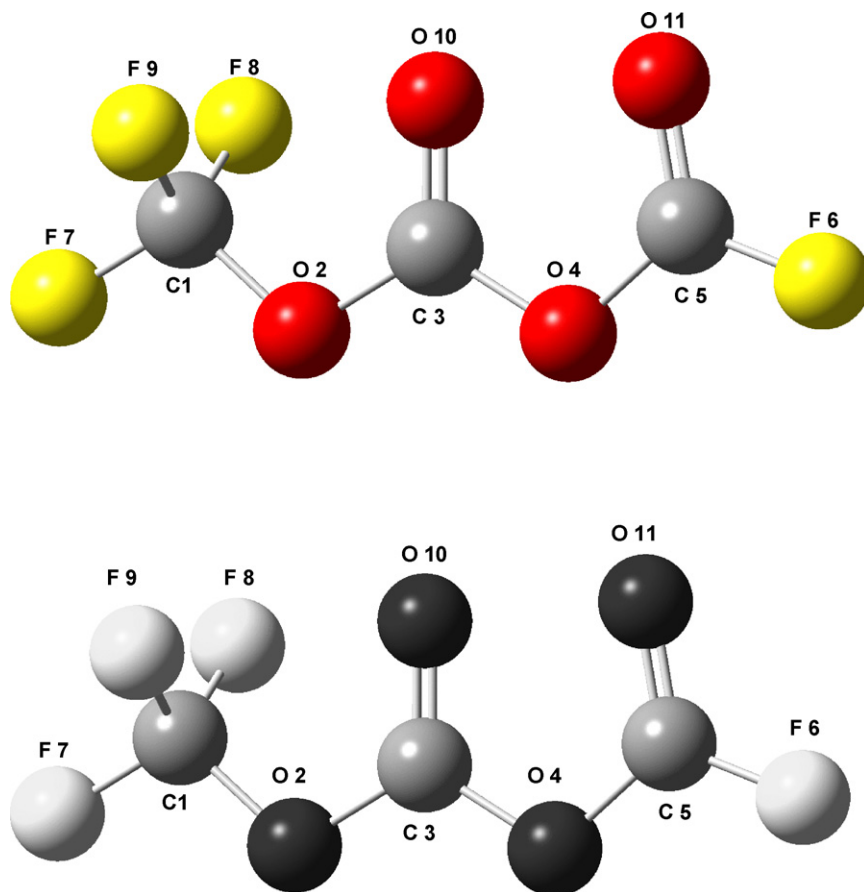


Fig. 2. Most stable conformer at the B3LYP/6-311+G* level.

Table 2

Geometrical parameters for $\text{CF}_3\text{OC}(\text{O})\text{OC}(\text{O})\text{F}$ (B3LYP/6-311+G*) and the related anhydrides $\text{FC}(\text{O})\text{OC}(\text{O})\text{F}$ [6] and $\text{CF}_3\text{OC}(\text{O})\text{OC}(\text{O})\text{OCF}_3$ [14]. Numbering of atoms follows from Fig. 1 and strictly applies only to $\text{CF}_3\text{OC}(\text{O})\text{OC}(\text{O})\text{F}$. The values informed for $\text{FC}(\text{O})\text{OC}(\text{O})\text{F}$ and $\text{CF}_3\text{OC}(\text{O})\text{OC}(\text{O})\text{OCF}_3$ are associations for the same type of bond or angle.

	$\text{CF}_3\text{OC}(\text{O})\text{OC}(\text{O})\text{F}$	$\text{FC}(\text{O})\text{OC}(\text{O})\text{F}$	$\text{CF}_3\text{OC}(\text{O})\text{OC}(\text{O})\text{OCF}_3^a$
Distances (Å)			
C–F	1.33	1.31	1.31
C1–O2	1.39		1.37
O2–C3	1.36		1.35
C3=O10	1.18	1.17	1.17
C3–O4	1.37	1.38	1.36
O4–C5	1.36	1.38	1.36
C5=O11	1.17	1.17	1.17
Angles (°)			
F–C–F	109.2		
F–C1–O2	106.0	105.0	106.4
C1–O2–C3	118.4		
O2–C3=O10	128.3	128.0	127.9
O2–C3–O4	103.9		103.5
C3–O4–C5	119.1	118.2	118.5
O4–C5=O11	129.2	128.0	127.9
F6–C5=O11	125.1		
O4–C5–F6	105.6	105.0	
Dihedrals (°)			
φ_0	179.3		179.1
φ_1	–2.4		
φ_2	–24.0		–13.7
φ_3	–21.1	20.8	–21.9

^a X-ray diffraction of a single crystal at -80°C

Table 1 shows the absolute (Hartree units) and relative plus ZPE (kcal mol^{-1}) energies of the most stable conformer as well as the relative population at 273 K.

Fig. 2 depicts the structure of the most stable calculated conformer. Bond lengths and angles are presented in Table 2 together with the experimental data available for the two related symmetrical anhydrides $\text{CF}_3\text{OC}(\text{O})\text{OC}(\text{O})\text{OCF}_3$ [6] and $\text{FC}(\text{O})\text{OC}(\text{O})\text{F}$ [14]. The geometrical parameters calculated agree with those observed in similar compounds. The most interesting features are those related with the $\text{O}=\text{C}-\text{O}-\text{C}=\text{O}$ fragment. In the present molecule the dihedrals $\text{O}=\text{C}-\text{O}-\text{C}=\text{O}$ and $\text{CF}_3\text{OC}-\text{O}-\text{C}=\text{O}$ are -24.0 and -21.1 degrees respectively, showing the syn-clinical conformation of both $\text{C}=\text{O}$ bonds found in others fluorinated anhydrides like $\text{CF}_3\text{C}(\text{O})\text{OC}(\text{O})\text{CF}_3$, $\text{FC}(\text{O})\text{OC}(\text{O})\text{F}$ and $\text{CF}_3\text{OC}(\text{O})\text{OC}(\text{O})\text{OCF}_3$. The corresponding dihedral is 20.8° in $\text{FC}(\text{O})\text{OC}(\text{O})\text{F}$ determined by gas

electron diffraction (GED). Unfortunately, there is no GED study of $\text{CF}_3\text{OC}(\text{O})\text{OC}(\text{O})\text{OCF}_3$ and the experimental values, -13.7 and -21.9° , result from the X-ray diffraction of the solid; however, the calculated value for both angles is 25.1° for the conformation in the gas phase. In the present case, the dissimilarity between φ_2 and φ_3 shows the different interactions of CF_3O and F with the carbonyl groups and parallels the tendency observed in the symmetrical anhydrides.

4.3. IR analysis

$\text{CF}_3\text{OC}(\text{O})\text{OC}(\text{O})\text{F}$ has 27 vibrational modes, all of which are IR active. All the conformers belong to the C_1 symmetry group. Table 3 shows the vibrational modes experimentally accessible with the instrument as well as the theoretical frequencies calculated for the s–s–s rotamer without any correction. The IR transitions for the symmetric anhydrides are also included for comparison. The carbonyl stretching vibrations in the asymmetric molecule are within the values for the symmetric ones, it can be seen that the average value for these vibrations are 1873 and 1905 cm^{-1} for $\text{FC}(\text{O})\text{OC}(\text{O})\text{F}$ and $\text{CF}_3\text{OC}(\text{O})\text{OC}(\text{O})\text{OCF}_3$ respectively and 1891 cm^{-1} for $\text{CF}_3\text{OC}(\text{O})\text{OC}(\text{O})\text{F}$. A similar effect is observed for the strongest vibrations, which mainly corresponds to stretching of the $\text{C}-\text{O}-\text{C}$ fragment; for the symmetric molecules the bands are at 1168 and 1057 cm^{-1} and the asymmetric is at 1116 cm^{-1} . This effect can be thought of as a transition of properties going from one to the other symmetric anhydride through the asymmetric one.

Fig. 1 shows the experimental IR spectrum of $\text{CF}_3\text{OC}(\text{O})\text{OC}(\text{O})\text{F}$ after subtraction of the remaining impurities together with a simulation. For the latter we used the B3LYP/6-311+G* frequencies (without corrections) and intensities of the three most stable rotamers at the populations in Table 1. Each vibrational transition was fitted with a Lorentzian profile using 2 cm^{-1} as FWHH, and the intensities were normalized for suitable comparison with the experimental spectrum. Taking into account the calculated absorption cross sections and the relative populations of the rotamers, the only transitions with quantitative differences are those corresponding to the carbonyl stretching. The values of ν_s and $\nu_{as} \text{ C}=\text{O}$ for the s–a–s and s–s–a rotamers (1936 – 1916 and 1956 – 1900 cm^{-1} respectively) are enclosed within the values belonging to the s–s–s rotamer (1968 – 1886 cm^{-1}), so a theoretical analysis of the spectra foresees a relatively wide and noisy asymmetric $\text{C}=\text{O}$ stretching when more than one rotamer is present in the sample. Inspection of the figure in the carbonyl region shows these features in the experimental and simulated

Table 3

Comparison of experimental and calculated (most stable conformer) mid-IR vibrational frequencies of $\text{CF}_3\text{OC}(\text{O})\text{OC}(\text{O})\text{F}$, and its parent symmetric molecules. Relative intensities higher than 10 are shown in brackets. Assignments are qualitative because of strong coupling.

$\text{CF}_3\text{OC}(\text{O})\text{OC}(\text{O})\text{F}$	Calculated ^a	$\text{FC}(\text{O})\text{OC}(\text{O})\text{F}$	$\text{CF}_3\text{OC}(\text{O})\text{OC}(\text{O})\text{OCF}_3$	Approximate description of mode
1922 (13.6)	1967.8 (29.9)	1941 (58)	1900 (15)	$\nu_1 \text{ C}=\text{O}$
1860 (4)	1885.7 (7.1)	1870 (8)	1846 (7)	$\nu_2 \text{ C}=\text{O}$
1297 (10.2)	1264.6 (7.71)			$\nu_3 \text{ F}_2\text{C}-\text{F}$
1260 (22.3)	1244.9 (10.2)		1293 (30)	$\nu_4 \text{ (O)C}-\text{O}-\text{C}(\text{O})$
	1215.6 (18.82)	1249 (25)	1259 (48)	$\nu_5 \text{ CF}_3$
	1208.2 (4.13)		1198 (5)	$\nu_6 \text{ CF}_3/\nu_{as} \text{ C}-\text{O}-\text{C}$
1116 (100)	1083.5 (100)	1168 (100)	1100 (67)	$\nu_7 \text{ C}-\text{O}-\text{C}(\text{O})/\nu_{as} \text{ (O)C}-\text{O}-\text{C}(\text{O})$
	1061.2 (11.62)	1030 (5)	1057 (100)	$\nu_8 \text{ C}-\text{O}-\text{C}(\text{O})/\nu_{as} \text{ (O)C}-\text{O}-\text{C}(\text{O})$
988 (1.7)	944.1 (1.3)	938 (6)	964 (2)	$\nu_9 \delta_s \text{ C}-\text{O}-\text{C}/\delta_s \text{ C}-\text{O}-\text{C}$
943 (1)	875.0 (1.08)		876 (1)	$\nu_{10} \nu_s \text{ CF}_3/\text{CF}_3-\text{O}$
	812.5			$\nu_{11} \delta_{as} \text{ C}-\text{O}-\text{C}/\delta_{as} \text{ C}-\text{O}-\text{C}$
765 (1.4)	768.3 (2.68)	765 (6)		$\nu_{12} \text{ oop s OOC}=\text{O}/\text{OFC}=\text{O}$
	742			$\nu_{13} \text{ oop as OOC}=\text{O}/\text{OFC}=\text{O}$
	708.2			$\nu_{14} \delta \text{ O}-\text{C}-\text{O}$
609 (2.9)	610.4 (1.2)	652 (8)		$\nu_{15} \delta \text{ CF}_3/\delta \text{ O}=\text{C}-\text{F}$

^a The following are the rest of the calculated frequencies that were not observed experimentally: $\nu_{16} 604.4$ (1.09), $\nu_{17} 559.9$, $\nu_{18} 471.8$, $\nu_{19} 428.1$, $\nu_{20} 379$, $\nu_{21} 288.3$, $\nu_{22} 227.5$, $\nu_{23} 140.9$, $\nu_{24} 110$, $\nu_{25} 88.2$, $\nu_{26} 48.9$, $\nu_{27} 38.2$.

spectra. For the remaining vibrations the theoretical spectra predicts a strong overlapping between the *s*–*s* rotamer and the other ones.

Three bands centred at 1264, 1245, and 1215 cm^{-1} appear in the simulated spectrum, which were observed as two in the experimental one (1297, 1260 cm^{-1}). This may be due to the fact that 1264 and 1245 frequencies are closer in the real spectrum so they appear as a single signal in the experimental one. A similar situation occurs at 1061 cm^{-1} of the simulated spectrum, where there is a shoulder for the strongest absorption which is not observed in the experimental one.

5. Conclusions

The synthesis and characterization of the new asymmetric anhydride $\text{CF}_3\text{OC}(\text{O})\text{OC}(\text{O})\text{F}$ have been accomplished through the combination of CF_3OCO and FCO_2 radicals produced in the thermal decomposition of $\text{CF}_3\text{OC}(\text{O})\text{OOC}(\text{O})\text{F}$ in excess of CO. The key to obtain the anhydride is the condensation of trioxide on the walls of the reactor, removing all other products and adding CO. In this way when the trioxide decomposes, the concentration of CF_3OCO and FCO_2 radicals is appropriate to form $\text{CF}_3\text{OC}(\text{O})\text{OC}(\text{O})\text{F}$ although with $\text{CF}_3\text{OC}(\text{O})\text{OC}(\text{O})\text{OCF}_3$ as impurity. Another method for the synthesis was the reaction between $\text{CF}_3\text{OC}(\text{O})\text{OOC}(\text{O})\text{F}$, $\text{FC}(\text{O})\text{OOC}(\text{O})\text{F}$ and CO, which prevents formation of $\text{CF}_3\text{OC}(\text{O})\text{OC}(\text{O})\text{OCF}_3$.

The conformational analysis performed using the B3LYP/6-311+G* hybrid method indicates that the *s*–*s* conformer is the most stable one, and that at room temperature the populations of the *s*–*s*, *s*–*a*–*s*, and *s*–*s*–*a* rotamers could be appreciable. The mid-IR experimental spectrum was simulated using the frequencies obtained from the B3LYP calculations for the three rotamers. Very good agreement can be found when comparing both results, and the presence of the three conformers in the experimental spectrum becomes evident when analyzing the carbonyl region.

Acknowledgments

Authors would like to thank CONICET, ANPCyT of Argentina, and SeCyT-UNC for financial support. Language assistance by translator R. Karina Plasencia is gratefully acknowledged.

References

- [1] D. DesMarteau, L. Changqing, *Journal of Fluorine Chemistry* 132 (2011) 1194–1197.
- [2] G. Kostov, B. Ameduri, T. Sergeeva, W.R. Dolbier Jr., R. Winter, G.L. Gard, *Macromolecules* 38 (2005) 8316–8320.
- [3] H. Pernice, H. Willner, K. Bierbrauer, M.A. Burgos Paci, G.A. Argüello, *Angewandte Chemie International Edition* 41 (2002) 3832–3834.
- [4] A.J. Arvia, P.J. Aymonino, C.H. Waldow, H.J. Schumacher, *Angewandte Chemie International Edition* 72 (1960) 169.
- [5] H. Pernice, M. Berkei, G. Henkel, H. Willner, G.A. Argüello, M.L. McKee, T.R. Webb, *Angewandte Chemie International Edition* 43 (2004) 2843–2846.
- [6] P. García, H. Willner, M.A. Burgos Paci, G.A. Argüello, T. Berends, *Journal of Fluorine Chemistry* 126 (2005) 984–990.
- [7] G.A. Argüello, H. Willner, F.E. Malanca, *Inorganic Chemistry* 39 (2000) 1195–1199.
- [8] S. von Ahsen, P. García, H. Willner, M.A. Burgos, G.A. Argüello, *Chemistry: A European Journal* 9 (20) (2003) 5135–5141.
- [9] M.A. Burgos, P. García, F.E. Malanca, H. Willner, G.A. Argüello, *Inorganic Chemistry* 42 (2003) 2131–2135.
- [10] M.D. Manetti, M.A. Burgos Paci, G.A. Argüello, *Journal of Physical Chemistry A* 113 (2009) 8523–8528.
- [11] H.G. Mack, C.O. Della Vedova, H. Oberhammer, *Angewandte Chemie International Edition* 103 (1991) 1166–1167.
- [12] M.A. Burgos Paci, P. García, H. Willner, G.A. Argüello, *International Journal of Chemical Kinetics* 35 (1) (2003) 15–19.
- [13] D. Hnyk, J. Macháček, G.A. Argüello, H. Willner, H. Oberhammer, *Journal of Physical Chemistry A* 107 (2003) 847–851.
- [14] F. Mayer, H. Oberhammer, M. Berkei, H. Pernice, H. Willner, K. Bierbrauer, M. Burgos Paci, G.A. Argüello, *Inorganic Chemistry* 43 (25) (2004) 8162–8168.
- [15] M.A. Burgos Paci, G.A. Argüello, P. García, H. Willner, *Journal of Physical Chemistry A* 109 (2005) 7481–7488.
- [16] C.W. Tullock, D.D. Coffman, *Journal of Organic Chemistry* 25 (1960) 2016–2019.
- [17] C.O. Della Vedova, R. Boese, H. Willner, H. Oberhammer, *Journal of Physical Chemistry A* 108 (2004) 861–865.
- [18] C. Lee, W. Yang, R.G. Parr, *Physical Review B* 37 (1988) 785–789.
- [19] M.J. Frisch, G.W. Trucks, H.B. Schlegel, G.E. Scuseria, M.A. Robb, J.R. Cheeseman, J. Montgomery, T. Vreven, K.N. Kudin, J.C. Burant, J. Millam, S.S. Iyengar, J. Tomasi, V. Barone, B. Mennucci, M. Cossi, G. Scalmani, N. Rega, G.A. Petersson, H. Nakatsuji, M. Hada, M. Ehara, K. Toyota, R. Fukuda, J. Hasegawa, M. Ishida, T. Nakajima, Y. Honda, O. Kitao, H. Nakai, M. Klene, X. Li, J.E. Knox, H.P. Hratchian, J.B. Cross, C. Adamo, J. Jaramillo, R. Gomperts, R.E. Stratmann, O. Yazyev, A.J. Austin, R. Cammi, C. Pomelli, J. Ochterski, P.Y. Ayala, K. Morokuma, G.A. Voth, P. Salvador, J.J. Dannenberg, V.G. Zakrzewski, S. Dapprich, A.D. Daniels, M.C. Strain, O. Farkas, D.K. Malick, A.D. Rabuck, K. Raghavachari, J.B. Foresman, J.V. Ortiz, Q. Cui, A.G. Baboul, S. Clifford, J. Cioslowski, B.B. Stefanov, G. Liu, A. Liashenko, P. Piskorz, I. Komaromi, R.L. Martin, D.J. Fox, T. Keith, M.A. Al-Laham, C.Y. Peng, A. Nanayakkara, M. Challacombe, P.M. Gill, B. Johnson, W. Chen, M.W. Wong, C.J.A. Gonzalez, J.A. Pople, Gaussian 03, Gaussian Inc., Pittsburgh, PA, 2003.
- [20] G. Schaftenaar, J.H. Noordik, *The Journal of Computer-Aided Molecular Design* 14 (2000) 123–134.
- [21] T.J. Wallington, M.D. Hurley, M. Mariqc, *Chemical Physics Letters* 205 (1993) 62–68.
- [22] M. Mariqc, J. Szenté, G. Khitrov, J. Fransisco, *Journal of Physical Chemistry* 100 (1996) 4514–4520.
- [23] M.A. Burgos Paci, P. García, H. Pernice, H. Willner, G.A. Argüello, *Journal of the Argentine Chemical Society* 93 (2005) 175–182.